Computers Math. Applic. Vol. 18, No. 5, pp. 439–448, 1989
Printed in Great Britain.

0097-4943/89 $3.00 + 0.00

MULTIPLE STEADY STATE HORIZONTAL BUOYANCY INDUCED FLOWS IN POROUS MEDIA SATURATED WITH COLD WATER

Y.-Y. CHEN and C.-A. WANG†

Institute of Applied Mathematics, National Chiao Tung University, Hsinchu, Taiwan 30050, R.O.C.

(*Received* 27 *September* 1988)

Abstract—A similarity boundary value problem which describes the steady-state buoyancy induced plane flow next to an impermeable, horizontal surface in porous media saturated with cold water is studied. Numerical solutions are found in two disjoint regions of temperature-ratio parameter R by using a multiple shooting code BVPSOL. In each region, solutions are obtained by applying the continuity process which gives, respectively, a smooth bifurcation curve in term of a appropriate parameter. Multiple solutions are found at some R in this two regions. Some of them are similar and others indicate physically the potential existence of a large amount of energy for any trend arising that drives one steady state to another.

NOMENCLATURE

f—similarity stream function
g—acceleration of gravity
I_W—total buoyancy force
K—permeability of porous medium
Nu_x—local Nusselt number
p—pressure of global enviroment
p_m—motion pressure
P—similarity function of motion pressure
q—exponent in density equation
R—temperature ratio
R^*—the lower bound of the gap in terms of R
R_*—the upper bound of the gap in terms of R
Ra_x—local Rayleigh number
t—temperature
t_m—temperature at which maximum density occurs for a given salinity and pressure
t_0—surface temperature
t_∞—ambient temperature
u—Darcy velocity in x-direction
v—Darcy velocity in y-direction
W—local buoyancy force defined in equation (12)
x—coordinate parallel to the surface
y—coordinate vertical to the surface
α_1—thermal diffusivity ratio of matrix conductivity to fluid heat capacity
η—non-dimensional distance in boundary region
η_∞—value of η at the edge of boundary region
κ—effective thermal conductivity of saturated porous medium
μ—dynamic viscosity
ρ—density
ρ_m—maximum density
ρ_∞—density of ambient fluid
ρ_r—reference quantity of density
φ—normalized temperature
ψ—stream function

1. INTRODUCTION

In the natural world, transport processes in fluids where the motion is driven by the interaction of a difference in density in a gravitational field are common. Usually, the density variation is caused by temperature differences and the density variation of pure and even of saline water at

†The author acknowledges support in part by National Science Council of R.O.C.

low temperatures often results in very complicated buoyancy induced flows. If an internal temperature variation arises which spans the temperature t_m at which a density extremum $\rho_m(t_m)$ arises, a buoyancy force reversal follows. This may lead to flow reversal and other complicated convective effect.

Early investigations of buoyancy induced flows were mainly concentrated on vertical laminar convective flows in water which were summarized in [1]. For example, consider a vertical surface at uniform temperature $t_0 = 8°C$, in a quiescent pure water ambient at $t_\infty = 2°C$. Near the surface, the fluid is less dense than the ambient and the buoyancy force is upward. However, the extremum of pure water at 1 atm occurs at about 4°C, the fluid in the outermost portion of thermal transport regions is more dense than the ambient consequently, the buoyancy force is downward. Combining these two results, the buoyancy force reversal across the thermal diffusion region occurs. As the situation intensifies, there is possibility of occurring "local flow reversal", i.e. the direction of the tangential velocity changes across the boundary layer region and even further to "convective inversion", i.e. the reversal of direction of net mass flow.

From above example, it is observed that if t_m lies between t_0 and t_∞, then a reversal in buoyancy force $g[\rho(t_\infty) - \rho(t)]$ arises across the thermal region, where g is the magnitude of the gravity force. The parameter that characterizes this temperature interrelation is

$$R = \frac{t_m - t_\infty}{t_0 - t_\infty}. \tag{1}$$

When $0 < R < 0.5$, a buoyancy force reversal arises.

Many recent evaluations use the density relation for pure and saline water given in [2]. This is a simple and accurate expression for the buoyancy force causing motion in low temperature pure and saline water. A number of recent theoretical and experiment studies have added considerable understanding of these complex flows for pure and saline water and for porous media saturated with pure and saline water. The boundary-layer calculation in [3] resulted in solutions in a gap from about $R = 0.15$ to $R = 0.30$. A similar gap was found for numerical solutions of time dependent Navier–Stokes equations in [4]. Then, in [5], solutions in [3] were extended to reduce the remaining gap to $R = 0.15180$–0.29181. Gebhart *et al.* [6] presented a more delicate numerical study to obtain new solution and improved the accuracy gap in R by appropriate parameters and multiple solutions with great different characteristics at the some R are found. Wang [7] considered a vertical ice wall melting in saturated porous media and similar results were obtained. These results were verified rigorously by Hastings and Kazarinoff [8] and Wang [9] respectively.

For the convective phenomenon of transport adjacent to a heated or cooled horizontal surface embedded in a porous medium saturated with water, early investigations are summarized in [10]. Lin and Gebhart [11] then used the density variation in [2] to present similarity analysis of transport in porous media saturated with cold water. In [11], existence of similarity solutions for the case of isothermal horizontal surface were reported under atomospheric pressure 1 bar absolute and numerical data seemed to indicate the uniqueness of solution at a given R. An interval $0.08 < R < 0.288$ was obtained on which no numerical similarity solution exists. In this paper, similar to [7], we present new solutions which exhibit existence of multiple solutions at some R in (0, 0.5) and obtain a more delicate gap, $0.082864 < R < 0.283270$, on which no steady state solution exists. Some of these solutions are similar and others give drastically different behaviors. Moreover, similar results are also obtained for the physically maximal allowable case at $p = 1000$ bar.

2. DERIVATION OF SIMILARITY BOUNDARY VALUE PROBLEM

The derivation of the steady, planar, boundary layer equations for porous media saturated with cold water is given in [11]. These equations for flow adjacent to a horizontal, impermeable, isothermal surface at temperature t_0 and lying at $x \geqslant 0$ and $y = 0$, as shown in Fig. 1, in a homogenous and isotropic medium at temperature t_∞ are as follows:

$$f'(\eta) - \tfrac{2}{3}\eta P'(\eta) + \tfrac{2}{3}P(\eta) = 0, \tag{2}$$

$$\phi''(\eta) + \tfrac{1}{3}f(\eta)\phi'(\eta) = 0, \tag{3}$$

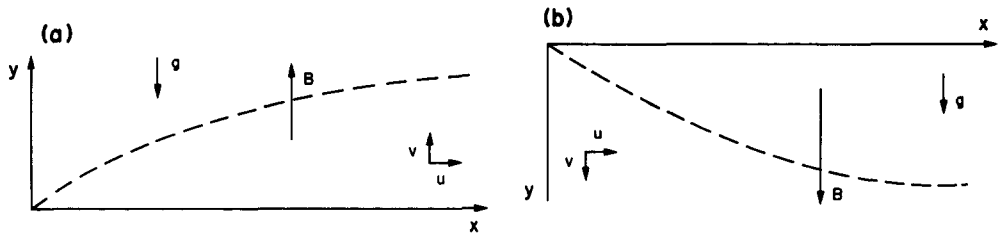

Fig. 1

$$P'(\eta) = W(\phi(\eta), R) = |\phi(\eta) - R|^q - |R|^q, \tag{4a}$$

$$P'(\eta) = -W(\phi(\eta), R) = |R|^q - |\phi(\eta) - R|^q, \tag{4b}$$

with boundary conditions

$$f(0) = \phi(0) - 1 = \phi(\infty) = P(\infty) = 0, \tag{5}$$

where equations (4a) and (4b) are corresponding to flows on the upper side and the bottom side of the horizontal surface, respectively. Furthermore, the total buoyancy force I_w out across the boundary region is defined by

$$I_w = \int_0^\infty W(\phi(\eta), R)\, d\eta.$$

This quantity is effective in indicating the net effect of buoyancy in the flow.

In [11], the following similarity transformation was given by defining the independent similarity variable η as

$$\eta(x, y) = \frac{y(\mathrm{Ra}_x)^{2/3}}{x} \tag{6a}$$

and similarity functions $f(\eta)$, $\phi(\eta)$, $P(\eta)$ by the correlations

$$\psi(x, y) = \alpha_1 f(\eta)(\mathrm{Ra}_x)^{1/3}, \tag{6b}$$

$$\phi(\eta) = \frac{t - t_\infty}{t_0 - t_\infty}, \tag{6c}$$

$$P_m(x, y) = \frac{\alpha_1 \mu (\mathrm{Ra}_x)^{2/3}}{Kx} P(\eta), \tag{6d}$$

where the local Rayleigh number Ra_x is defined by

$$\mathrm{Ra}_x = \frac{\alpha K \rho_m g |t_0 - t_m|^q x}{\mu \alpha_1}, \tag{6e}$$

and ψ denotes the stream function satisfying $\psi_y = u(x, y)$ and $-\psi_x = v(x, y)$. The constant quantity α, K, μ, q and α_1 are the thermal diffusivity, permeablility, viscosity, and exponent and constant in the density relation, respectively. Moreover, u and v are the tangential and normal component of Darcy velocity and p_m represents the motion pressure of the fluid.

From the transformation, $f'(\eta)$ is proportional to the tangential velocity while $f(\eta) - 2\eta f'(\eta)$ is proportional to the normal velocity satisfying

$$\psi_y = \frac{\alpha_1 (\mathrm{Ra}_x)^{2/3} f'}{x}, \qquad v = -\psi_x = \frac{\alpha_1 (\mathrm{Ra}_x)^{1/3}}{3x}(f - 2\eta f').$$

Furthermore, $P(\eta)$ is proportional to the motion pressure and $\phi(\eta)$ is proportional to the temperature profiles with $-\phi'(0)$ relating to the rate of heat transfer at the surface, i.e. $-\phi'(0)$ is proportional to $\mathrm{Nu}_x = q'' x/((t - t_\infty)\kappa)$ where q'' is the surface heat flux and Nu_x is the local Nusselt number.

For convenience, BVP$^+$ denotes the problem which consists of equations (2), (3), (4a) and conditions (5), and BVP$^-$ denotes the problem of equations (2), (3), (4b) and conditions (5).

3. NUMERICAL STUDY AND RESULTS

For the numerical computation, the code BVPSOL [12–14], which solves general two-point boundary value problems by multiple-shooting method, is chosen. In fact, the shooting method consists of an initial value problem with some free parameters and a corresponding root finding problem for the conditions to be shot. Therefore, the shooting process mainly depends on the sensitivity of the integrator imposed for solving the initial value problem. For dealing with the stiff problem BVP, an efficient code METAN1 [15, 16], which is a semi-implicit midpoint integrator, is chosen. However, the length of problem domain may further affect the shooting scheme with a simple shooting. Thus, with imposed multiple shooting, such sensitivity effects will be reduced.

Moreover, equation (3) is equivalent to

$$\varphi'(\eta) = \varphi'(0)\exp\left(-\frac{1}{3}\int_0^{\eta} f(s)\,ds\right). \tag{7}$$

It can be shown that $\varphi'(\eta)$ tends to zero and $f(\eta)$ cannot be negative as η approaches infinity. Otherwise, either $\varphi(0) = 1$ or $\varphi(\infty) = 0$ will be violated. Also, the associated conditions for problem BVP are designated at the horizontal surface $\eta = 0$ and the far ambient region as η tending to infinity. Due to the finite nature for numerical computation, the far ambient boundary conditions can only be set at $\eta = \eta_\infty$ where η_∞ is finite. Then the reduced problem with finite domain $[0, \eta_\infty]$ is computed by BVPSOL with an accuracy controlling parameter EPS = 1.E − 8. Therefore, it is natural to say that numerical data is acceptable if $f(\eta_\infty)$ does not change for first six digits and $-\varphi'(\eta_\infty)$ is positive and less than 1.E − 6 when η_∞ is increase twice consecutively. Meanwhile, the buoyancy force term $W(\varphi(\eta), R)$, $\eta \geqslant 0$, can only change sign once for each R in (0, 0.5). Due to the interest of buoyancy force and flow reversal, numerical study of problem BVP are given on the region R in [0, 0.5]. All numerical computations are performed on Cyber 730 at NCTU.

To solve problem BVP$^+$ with $q = 1.894816$ under $p = 1$ bar, we apply the continuation scheme by starting R equals to 0 and increase R by a step size ΔR. Linear extrapolation of the solution obtained for R_1 and $R_2 (R_1 < R_2)$ is applied to provide the initial guess in BVPSOL for computing the solution at $R = R_3$ with $R_3 > R_2$ and ΔR halving scheme is also implemented if the initial guess gives failure of convergence in BVPSOL. Therefore, the largest R, say $R^* \approx 0.082864$, is reached at which numerical solution is obtained successfully. Note that our data R^* is beyond the upper bound $R = 0.08$ obtained by Lin and Gebhart [11]. On the botton side of the surface, problem BVP$^-$, we start at $R = 0.5$ and decrease R. By similar technique, the smallest R, say $R_* \approx 0.283270$ is obtained.

Moreover, as in [7], the continuation scheme should be able to continued if an additional equation

$$R' = 0 \tag{8}$$

and a proper boundary condition for a new free parameter are imposed. From the solution data obtained from problem BVP$^+$, it is observed that $f(\infty)$ decreases as R increases. Also, as mentioned earlier, $f(\infty)$ cannot be negative. Hence, it is proper to choose f_∞ as a free parameter and set the new boundary condition as $f(\eta_\infty) = f_\infty$. Correspondingly, the acceptance criterion in our program is adjusted to require the convergence of R instead of $f(\infty)$. The continuation method is then applied by reducing f_∞ from 1.4. The smallest successful level of f_∞ in our computation is 10^{-3} which gives η_∞ to be 1410. Compare with the case of $f_\infty = 10^{-2}$ with final η_∞ equals 430, it is reasonable to stop our continuity process for the case of f_∞ less than 10^{-3} since η_∞ will be too large to give acceptable data. On the bottom side of surface, problem BVP$^-$, similar observations from numerical data and from equation (7) give that $\varphi'(0)$ increases as R decreases and $\varphi'(0)$ must be negative. Therefore, an additional boundary condition $\varphi'(0) = \varphi_0'$ for problem P$^-$ is imposed and φ_0' is increased from -0.20. The largest successful level of φ_0' is -5×10^{-7} in our computation with final η_∞ equal to 120.

For the case of maximum of physically allowable $q = 1.582950$ at $p = 1000$ bar, similar scheme is also applied. For problem BVP$^+$, the largest R, $R^* \approx 0.067730$, is obtained when $f_\infty \approx 0.67039$ and a continuous family of solutions is successfully obtained for f_∞ reaching 0.006. For problem BVP$^-$, we obtain a lowest R, $R_* \approx 0.272195$ and a continuous family of solution is obtained for φ_0' tending to -0.00001.

Selected solutions data are shown in Tables 1–4. The bifurcation diagram of $f(\infty)$ vs R and $-\varphi'(0)$ vs R are plotted in Figs 2 and 3 respectively. Moreover, the profiles of temperature distribution φ, tangential velocity f', normal velocity $f-2\eta f'$, motion pressure P and local

Table 1. Selected solution data for problem BVP$^+$ with $q = 1.894816$ which are corresponding to flows near the upper side of horizontal surface

R	$f(\infty)$	$-\varphi'(0)$	$P(0)$	I_w
0	1.730841	0.341806	−1.210213	1.210213
0.02	1.595539	0.331237	−1.160720	1.160720
0.04	1.433235	0.319587	−1.109832	1.109832
0.061532	1.2	0.305397	−1.053757	1.053757
0.073670	1.0	0.296095	−1.021641	1.021641
0.080540	0.8	0.289736	−1.003261	1.003261
0.082849	0.6	0.286404	−0.996773	0.996773
0.082864†	0.58	0.286232	−0.996678	0.996678
0.082593	0.5	0.285820	−0.997129	0.997129
0.081636	0.4	0.285864	−0.999219	0.999219
0.080256	0.3	0.286389	−1.002318	1.002318
0.079533	0.25	0.286757	−1.003938	1.003938
0.078878	0.2	0.287136	−1.005395	1.005395
0.078371	0.15	0.287466	−1.006507	1.006507
0.078128†	0.012	0.287703	−1.006982	1.006982
0.078133	0.01	0.287701	−1.006971	1.006971
0.078145	0.005	0.287693	−1.006942	1.006942
0.078150†	0.003	0.287690	−1.006931	1.006931
0.078118	0.001	0.287700	−1.007012	1.007012

†Turning point.

Table 2. Selected solution data for problem BVP$^-$ with $q = 1.894816$ which are corresponding to flows near the bottom side of horizontal surface

R	$f(\infty)$	$-\varphi'(0)$	$P(0)$	I_w
0.5	2.633815	0.349146	−0.838122	−0.838122
0.441174	2.507626	0.320569	−0.656654	−0.656654
0.391176	2.387405	0.290569	−0.479821	−0.479821
0.351893	2.282377	0.260569	−0.316282	−0.316282
0.322215	2.195896	0.230569	−0.165267	−0.165267
0.301266	2.131867	0.200569	−0.026000	−0.026000
0.288404	2.095223	0.170569	0.102233	0.102233
0.283270†	2.098054	0.130569	0.256985	0.256985
0.288599	2.148667	0.100569	0.361029	0.361029
0.318854	2.371413	0.050569	0.507286	0.507286
0.342646	2.550374	0.030569	0.550020	0.550020
0.383290	2.891454	0.010569	0.564387	0.564387
0.401147	3.067369	0.005569	0.551862	0.551862
0.429584	3.417850	0.001194	0.507121	0.507121
0.438473	3.559856	0.000569	0.485999	0.485999
0.452033	3.834767	0.000109	0.446050	0.446050
0.459138	4.024362	0.000029	0.420951	0.420951
0.465044	4.220410	6.5E − 6	0.397608	0.397608
0.471861	4.512999	5E − 7	0.367368	0.367368

†Turning point.

Table 3. Selected solution data for problem BVP$^+$ with $q = 1.5822950$ which are corresponding to flows near the upper side of horizontal surface

R	$f(\infty)$	$-\varphi'(0)$	$P(0)$	I_w
0.	1.983775	0.366479	−1.304618	1.304618
0.01	1.874413	0.360467	−1.276721	1.266721
0.02	1.761326	0.353982	−1.247719	1.247719
0.03	1.639863	0.347083	−1.218047	1.218047
0.033073	1.6	0.344873	−1.208813	1.208813
0.039751	1.507578	0.339910	−1.188573	1.188573
0.051851	1.307578	0.330198	−1.151266	1.151266
0.060758	1.10	0.322095	−1.123129	1.123129
0.065834	0.90	0.316336	−1.105866	1.105866
0.067141	0.80	0.314682	−1.101770	1.101770
0.067698	0.70	0.313419	−1.099331	1.099331
0.067730†	0.67	0.313156	−1.099000	1.099000
0.067586	0.60	0.312742	−1.098871	1.098871
0.066963	0.505	0.312598	−1.099957	1.099957
0.063090	0.12	0.314586	−1.109021	1.109021
0.063033†	0.07	0.314660	−1.109153	1.109153
0.063033†	0.02	0.314630	−1.108980	1.108980
0.063120	0.011	0.314619	−1.108932	1.108932
0.063122†	0.010	0.314618	−1.108923	1.108923
0.063091	0.00575	0.314628	−1.109005	1.109005

†Turning point.

Table 4. Selected solution data for problem BVP$^-$ with $q = 1.582950$ which are corresponding to flows near the bottom side of horizontal surface

R	$f(\infty)$	$-\varphi'(0)$	$P(0)$	I_w
0.5	2.712113	0.365802	−0.918362	−0.918362
0.48	2.681665	0.357744	−0.860890	−0.860890
0.46	2.649700	0.349062	−0.800590	−0.800590
0.44	2.616065	0.339653	−0.737099	−0.737099
0.403226	2.549261	0.32	−0.610342	−0.610342
0.371872	2.486395	0.30	−0.488942	−0.488942
0.334536	2.403090	0.27	−0.319911	−0.319911
0.307064	2.335426	0.24	−0.165057	−0.165057
0.288066	2.286803	0.21	−0.022980	−0.022980
0.287076	2.284332	0.208	−0.013933	−0.013933
0.273650	2.258403	0.1655	−0.166556	−0.166556
0.272196†	2.266230	0.1455	−0.244066	−0.244066
0.273846	2.289299	0.1255	−0.316972	−0.316972
0.287222	2.392117	0.0855	−0.448474	−0.448474
0.310562	2.556384	0.053	−0.538196	−0.538196
0.371772	3.024104	0.013	−0.598783	−0.598783
0.417993	3.496970	0.002	−0.552538	−0.552538
0.442967	3.890071	0.00025	−0.493177	−0.493177
0.458349	4.268071	0.00002	−0.441336	−0.441336
0.461187	4.359901	0.00001	−0.430257	−0.530257

†Turning point.

buoyancy force W for various solutions of problem BVP with $q = 1.894816$ are also plotted in Figs 4–8 with data obtained by integrating equations (2)–(4) with METAN1.

By observing the bifurcation diagrams (Figs 2 and 3), it can be conjectured as follows:

Conjecture C1. There exist two numbers $R^*(q)$ and $R_*(q)$, $0 < R^*(q) < R_*(q) < 0.5$, such that problem BVP$^+$ has no solution for $R > R^*(q)$ and problem BVP$^-$ has no solution for $R < R_*(q)$. In particular, neither problem has a solution for $R^*(q) < R < R_*(q)$.

Conjecture C2. Problem BVP$^+$ has unique solution for each $R \geqslant 0$ and sufficiently small.

Conjecture C3. Let Γ be the solution set of BVP$^+$ for R in R in $[0, R^*]$. Then Γ is a smooth curve in the quadrant $R \geqslant 0$, $\alpha \geqslant 0$ that is of the form $R(\alpha)$, $0 \leqslant \alpha \leqslant \alpha_0$, where α_0 is the value of $f(\infty)$ corresponding to unique solutions at $R = 0$.

Conjecture C4. Corresponding to the curve Γ, there exists an infinite spiral curve in the quadrant $R \geqslant 0$ and $-\varphi'(0) \geqslant 0$ which is toward a point $(-\bar{\varphi}'(0), \bar{R}(q))$ where $(-\bar{\varphi}'(0), \bar{R}(q))$, $0 < \bar{R}(q) < R^*(q)$, is corresponding to a solution of problem BVP$^+$ when $f(\infty) = 0$. This indicates the existence of infinitely many solutions for problem BVP$^+$ at $R = \bar{R}(q)$.

Conjecture C5. Problem BVP$^-$ has a pair of solutions for each R, $R_*(q) < R < 0.5$ and has unique solution for each $R \geqslant 0.5$.

Conjectures C3 and C4 are made due to the fact of Crandall and Rabinowitz [17] that a bifurcation curve can only be terminated at a bifurcation point or reaching the boundary of

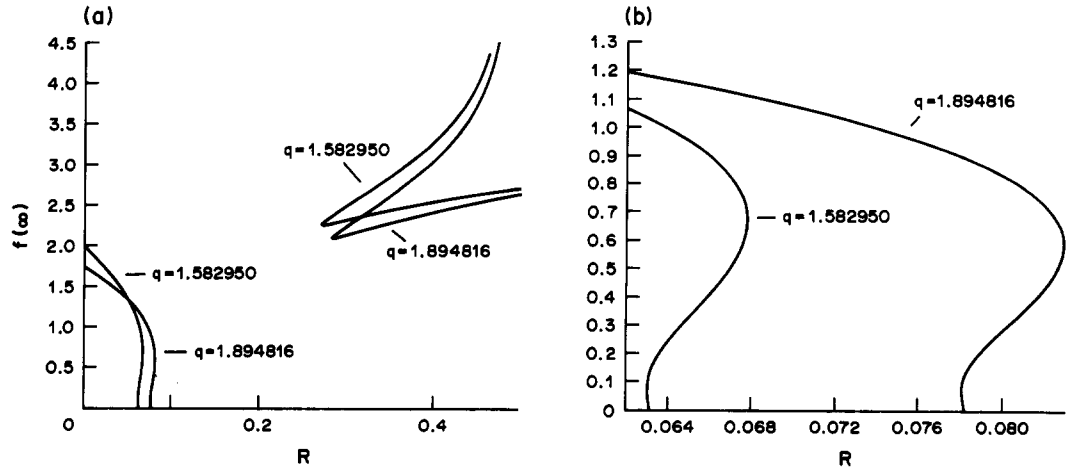

Fig. 2

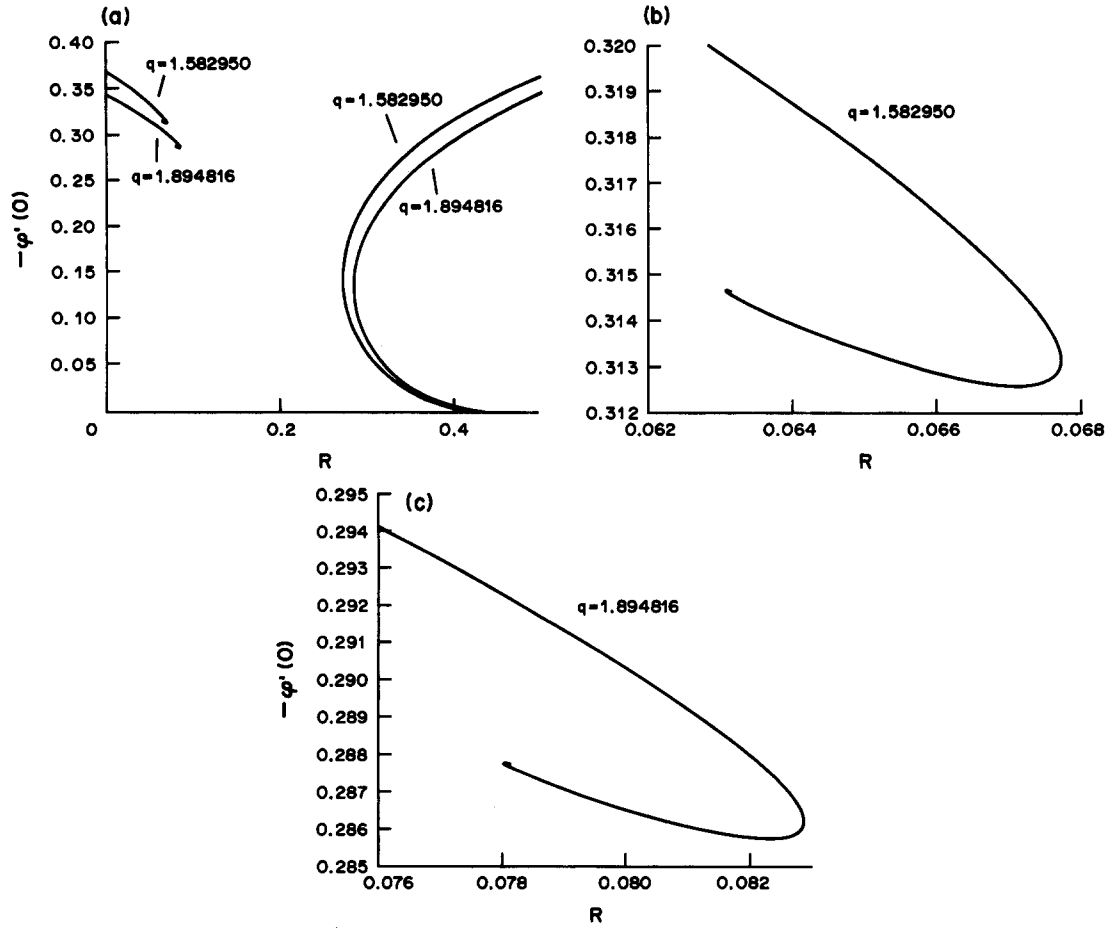

Fig. 3

problem domain. Although our computations do not present such terminology clearly, the left-hand branch in Fig. 2 should terminate at a point when $f(\infty) = 0$ while the right-hand lower branch for the problem BVP$^-$ should be sufficiently close to the point $(-\varphi'(0), R) = (0, .5)$ which is not corresponding to any solution of problem BVP$^-$. It should be noted here that verification of conjecture is not available. However, similar conjectures had been made for studies of vertical

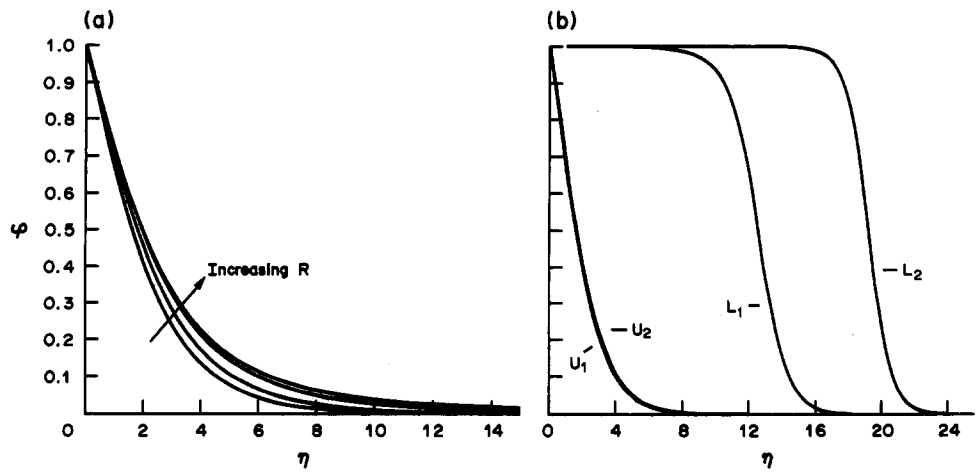

Fig. 4

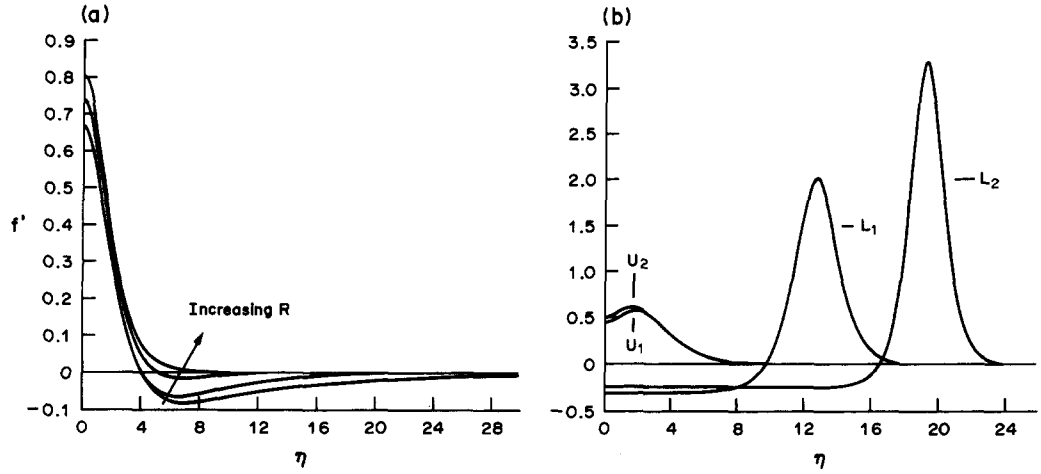

Fig. 5

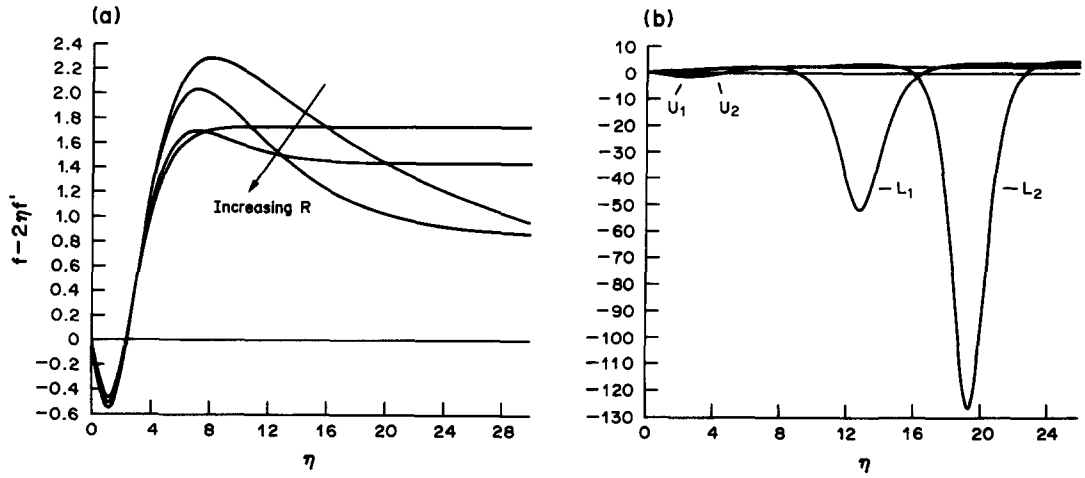

Fig. 6

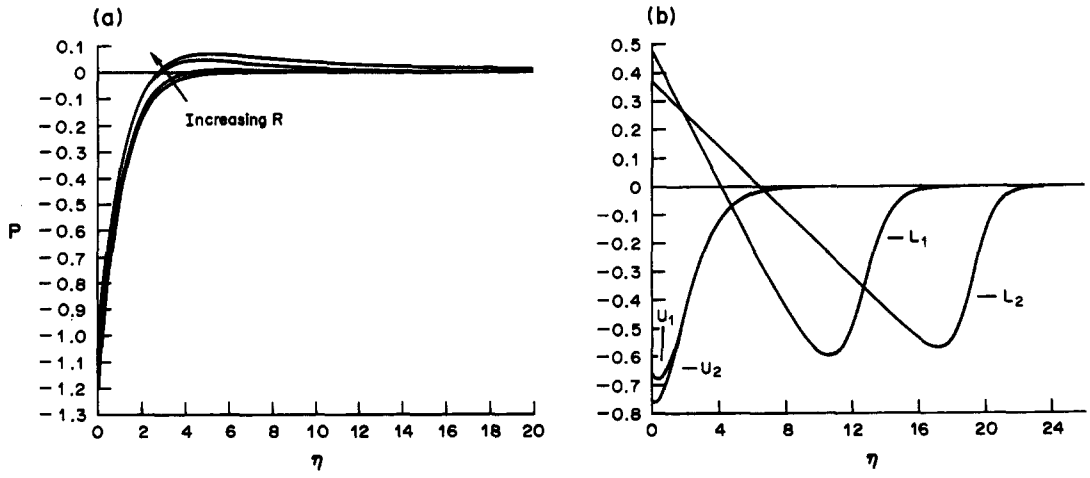

Fig. 7

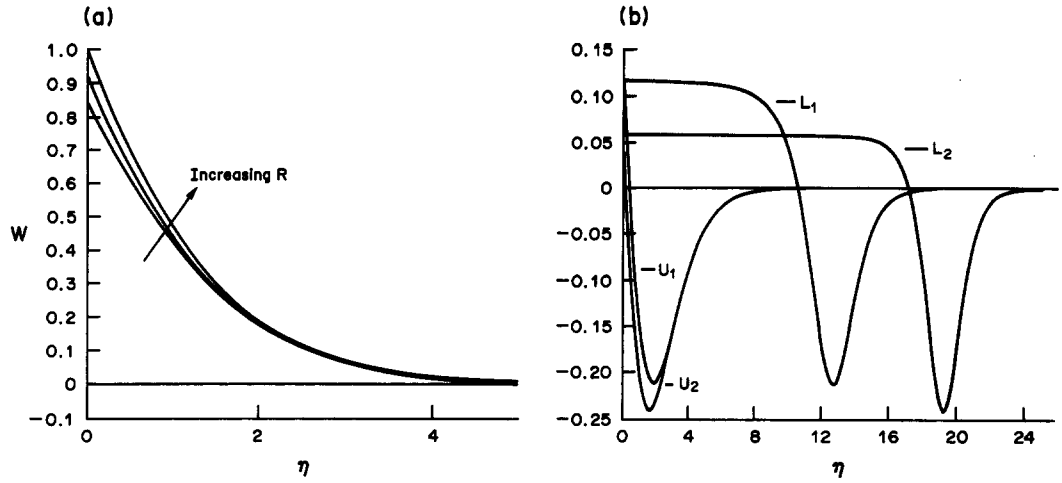

Fig. 8

transport as in [6] and [7], and corresponding mathematical verifications were also provided by Hastings and Kazarinoff [8] and Wang [9].

4. FURTHER OBSERVATIONS AND CONCLUSION

The numerical results presented in this paper may clarify several aspects of transports in the temperature-ratio parameter range $0 < R < 0.5$. In such range, buoyancy force and flow reversal arise along with convection inversion. As shown in Fig. 7a, the local buoyancy force W changes sign from negative across thermal region at large value of η for $0 < R < R^*(q)$. This exhibits an outside buoyancy force reversal. For the other range $R_*(q) < R < 0.5$, as in Fig. 7b, W changes sign at inner part of convective region, it is an inside buoyancy force reversal.

In the gap obtained, about $0.082849 < R < 0.283270$ for $q = 1.894816$ and $0.0677304 < R < 0.272195$ when $q = 1.582950$, no solution is obtained. Figure 2a shows that the lower and upper bounds vary weakly with q. Although no mathematical verification is given, it is conjectured from [8] and [9] that similar gap may exist for $q > 1$. However, the boundary layer approximation for equations (2)–(4) gives no indication in predicting the transport for R lies in the gap. A new formulation guided from new experimental study is necessary to describe such flows.

On the upper side of the surface, as shown in Figs 4–6, multiple solutions which coincide at the same R are very similar. The value of $-\varphi'(0)$ in Tables 1 and 2 further corroborates their similarity. On the other side of the surface, one of the pair of solutions is drastically different from the other. The lower solution clearly exhibits a thick layer of nearly stational flow adjacent to the surface. Physically, the existing boundary layer may insulate the horizontal surface and, consequently, reduce the rate of heat transfer. For example, at $R = 0.471861$, $-\varphi'_L(0)$ for the lower solution, which is related to the rate of heat transfer gives about 5×10^{-7}. However, the upper solution at the same R gives $-\varphi'_U(0)$ about 0.336176 and the quotient $-\varphi'_U(0)/-\varphi'_L(0)$ is about 6.6×10^5.

Consequently, multiple solutions for R lies in two regions $0 < R < R^*(q)$ and $R_*(q) < R < 0.5$ thus have considerably different characteristics. This raises additional questions in interpreting such results, in relation to any actual circulation in porous medium. Which flow might actually arise matters little in the left region, although the existence of multiple solutions probably means enhanced instability. However the differences in the effects of transport of solutions in the other region would be great. For example the large differences in temperature distributions mean large differences in the buoyancy force associated with the different flow at the same R. This indicates that a large amount of energy is potentially available for amplification of disturbances and vigorous effect may arise for driving a steady state to another.

Unfortunately, the data base from experimental measurement is meager concerning transport in porous media generally. Therefore, further surmises concerning flow instability and more inclusive modeling may require an experimental data base.

REFERENCES

1. B. Gebhart and J. C. Mollendorf, Buoyancy-induced flow in water under conditions in which density extremum may arise. *J Fluid Mech.* **89,** 673–707 (1978).
2. B. Gebhart and J. C. Mollendorf, A new density relation for pure and saline water. *Deep-Sea Res.* **24,** 813–848 (1977).
3. V. P. Carey, B. Gebhart and J. C. Mollendorf, Buoyancy force reversals in vertical nature convection flow in water. *J. Fluid Mech.* **97,** 279–297 (1980).
4. N. W. Wilson and J. J. Lee, Melting of a vertical ice wall by free convection into fresh water. *ASME J. Heat Transfer* **103,** 13–17 (1981).
5. El-Henawy, B. Gebhart, B. Hassard, N. Kazarinoff and J. C. Mollendorf, Numerically computed multiple steady states of vertical buoyancy-induced flows in cold pure water. *J. Fluid Mech.* **122,** 235–250 (1982).
6. B. Gebhart, B. Hassard, S. P. Hastings and N. Kazarinoff, Multiple steady-state solutions for buoyancy-induced transport in porous media saturated with cold pure or saline water. *Numer. Heat Transfer* **6,** 337–352 (1983).
7. C. A. Wang, Multiple numerical solutions of buoyancy induced flows of a vertical ice wall melting in saturated porous media. *Comput. Math. Applic.* **14,** 527–540 (1987).
8. S. P. Hastings and N. D. Kazarinoff, Multiple solutions for a problem in buoyancy-induced flow. *Archs rational mech. Analysis* **89,** 229–249 (1987).
9. C. A. Wang, Multiple solutions of problems of ice melting in porous media. *Tanking J. Math.* **19,** No. 1 (1988).
10. P. Cheng and L.-D. Chang, Buoyancy induced flows in a saturated porous medium adjacent to impermeable horizontal surfaces. *Int. J. Heat Mass Transfer* **19,** 1267–1272 (1976).
11. D. S. Lin and B. Gebhart, Buoyancy-induced flow adjacent to horizontal surface submerged in porous medium saturated with cold water. *Int. J. Heat Mass Transfer* **29,** 611–622 (1986).
12. P. Deuflhard, *Recent Advances in Multiple Shooting Techniques in Computational Techniques for Ordinary Differential Equations* (Ed. Gladwell/Sayers), Section 10, pp. 217–272. Academic Press, London (1980).
13. P. Deuflhard and G. Bader, Multiple shooting techniques revisited. Univ. Heidelberg, SFB 123 Tech. Rep. 163 (1982).
14. P. Deuflhard, A modified newton method for solution of ill condition system of the nonlinear equations with application to multiple shooting. *Numer. Math.* **22,** 289–315 (1974).
15. G. Bader and P. Deufihard, A semi-implicit midpoint rule for stiff systems of ordinary differential equations. University of Heidelberg, SBF 123 Tech. Rep. 114 (1981).
16. P. Deuflhard, Order and stepsize control in extrapolation methods. University of Heidelberg, SBF 123 Tech. Rep. 93 (1980).
17. M. G. Crandall and P. H. Rabinowitz, Bifurcation, perturbation of simple eigenvalue and linearized stability. *Archs rational mech. Analysis* **52,** 161–180 (1973).